Furthering information from OH and HO_2+RO_2 observations using a high resolution time of flight mass spectrometer

R.L. Mauldin III[1,2] , M.P. Rissanen[1], T. Petäjä[1], and M. Kulmala[1]

[1] Department of Physics, University of Helsinki, P.O. Box 64, 00014, Finland

5   [2] Department of Atmospheric and Oceanic Sciences, University of Colorado, Boulder, Colorado

Correspondence to: R.L. Mauldin (roy.mauldin@colorado.edu)

Abstract. An instrument has been developed which allows an entire suite of oxidation products (H_2SO_4 and highly-oxidized multifunctional compounds, HOMs) to be measured along with the concentrations of the key radical species OH and

10   HO_2+RO_2. The system combines the techniques for chemical conversion of OH or HO_2+RO_2 into H_2SO_4 together with nitrate ion (NO_3^-) Chemical Ionization (CI) and Atmospheric Pressure interface - Time of Flight Mass Spectrometer (NO_3^- CI-APi-ToF) which has been previously used for the detection of HOMs and a few other oxygenated organic species. The system exhibits the same sensitivity towards OH or HO_2+RO_2 as previous quadrupole chemical ionization (CIMS) measurements with limits of detection of ~2 x 10^5 and ~2 x 10^6 molecule cm^{-3} for OH and HO_2+RO_2 respectively. Unlike

15   previous CIMS measurements, the use of a NO_3^- CI-APi-ToF allows the acquisition of the entire mass spectrum at high resolution with each measurement, allowing one to see how the organic species behave when the sample flow is perturbed with reagent gasses (SO_2 or NO). While the combination of these measurements into one instrument is of great practical value, it is the combination of these data within the spectra obtained in each mode that extends the information far beyond the measurements themselves.

20   **1 Introduction**

Oxidation is a central atmospheric process and impacts such issues as climate change, air quality, and acid rain. Key here are reactions involving the hydroxyl radical (OH), the hydroperoxy radical (HO_2), and organic peroxy radicals (RO_2). OH reacts with volatile organic compounds (VOCs) usually leading to the formation of organic peroxy radicals, which in the presence of nitric oxide (NO) primarily regenerate OH. This fast cycling of radicals, which results in chemical lifetimes of OH less

25   than one second, controls many aspects of atmospheric chemistry such as the formation of ozone and secondary organic aerosols, and the removal of methane and other greenhouse gases such as halocarbons that affect the radiative balance of the atmosphere. Because of this central role, measurements of these radicals can provide a critical test of our understanding of the fast photochemistry of the atmosphere, as the concentration of OH in the atmosphere is determined by the chemistry of VOCs and NO_x rather than the result of transport (Heard and Pilling, 2003).

1

Towards these ends, two techniques have emerged as the most commonly used for the detection of peroxy radicals and OH. One technique, often referred to as FAGE (Fluorescence Assay by Gas Expansion), involves the laser induced fluorescence, LIF, detection of OH. HO_2 is measured by first converting it to OH which is subsequently detected. The other technique, utilized in this work, involves the addition of reagent gases to the sample flow causing the chemical conversion of the radical

5   species into sulfuric acid, H_2SO_4, which is subsequently detected via nitrate ion (NO_3^-) chemical ionization mass spectrometry, CIMS. By changing the species or concentration of the added reagents (NO, SO_2, propane) it is possible to measure ambient concentrations of OH, HO_2, and HO_2+RO_2, as well as ambient H_2SO_4.

While the NO_3^- ion CIMS has been in use for decades, the limitations of a quadrupole mass spectrometer have mainly limited its use to the measurement of H_2SO_4. Recently, NO_3^- ion chemical ionization has been coupled to an APi-TOF mass

10   spectrometer and is proving to be a highly valuable measurement on its own. Jokinen et al. (2012) have used the NO_3^- CI-APi-ToF technique to measure sulfuric acid clusters. It has since been used it to examine the formation of highly-oxidized multifunctional compounds, HOM, species (Ehn et al. ,2014; Jokinen et al., 2014; Rissanen et al. 2014, 2015).

Here we describe a single instrument capable of measuring OH, HO_2+RO_2, H_2SO_4 and other species detectable by nitrate chemical ionization. It employs two modes where reagent gasses are added to the sample, for the separate determination of

15   OH and HO_2+RO_2, and third NO_3^- ion mode where no reagent gases are added. While the use of one instrument to perform these measurements is practical, the fact that the spectra are all obtained with the same instrumental constraints (calibration, resolution, transmission, etc.) allows for accurate intercomparison of spectra obtained in each mode. Observing the behavior of the spectrum as whole under the varying conditions where reagent gasses are added or not, chemical data can be obtained towards the identity of many of the organic peaks observed, thus furthering the information gained beyond the individual

20   OH, and HO_2+RO_2 measurements by themselves.

2 Instrumentation

A schematic of the instrument is shown in Figure 1. The instrument combines the techniques of CIMS OH developed by Eisele et al. (1991, 1993) where SO_2 is added to the sample flow, and the HO_2+RO_2 technique described by Edwards et al. (2003), where SO_2 and NO are added to the sample flow, with the additional extension of High Resolution Time of Flight

25   mass detection. Briefly, the instrument can be operated in three different modes: One for the detection of hydroxyl radicals (OH mode), one for the detection of peroxy radicals (HO_2+RO_2 mode), and one where the sample flow is not treated with reagent compounds (NO_3^- mode). These modes allow the sequential determination of [OH], [HO_2+RO_2], [H_2SO_4], an upper limit to the concentration of other SO_2 oxidants as well as numerous compounds which have been previously identified as highly-oxidized multifunctional compounds or HOMs. The combination of OH and HO_2+RO_2 measurements has been

30   performed before using a quadrupole mass spectrometer (Sjostedt et al., 2007; Mauldin et al., 2004). The HO_xRO_x instrument described here extends these abilities with the addition of the NO_3^- ion mode and the use of HR ToF detection. To the author's knowledge, this is the first use of an HR ToF for either OH or HO_2+RO_2 measurements. As will be pointed out

below, the combination of these features allows more information to be gained than just the measurement of the individual concentrations.

Measurements were performed during April-May 2014 at the Hyytiälä research station located in the boreal forest approximately 200 km north of Helsinki, Finland. The instrument was located in a trailer with the inlet extending ~30 cm beyond the southern facing wall. Ambient air was drawn in via a 10.1 cm ID inlet with a flow velocity of ~2.5 m s^{-1}. Air is sampled from the central portion of this flow into the instrument via a 1.9 cm ID OD stainless steel tube (wall thickness ~0.01 cm). Depending upon the measurement mode, reagent compounds are added to this sample flow before entering the ion reaction region (see Figure 1). Details of the chemistry of each mode are given below.

2.1 NO_3^- Mode

The NO_3^- mode is the simplest operating mode where no reagent gasses are added to the sample flow. This mode also forms the basis of detection and quantification of H_2SO_4 (detected as HSO_4^- and $HNO_3 \cdot HSO_4^-$) formed from the other modes. The technique has been described previously for the use with a quadrupole mass spectrometer (Eisele et al., 1991, 1993; Mauldin et al., 1998; Petäjä et al., 2009) and more recently with a High Resolution Time of Flight mass spectrometer (Jokinen et al., 2012). The front end is of the same design and dimensions as that used by Eisele and Mauldin, and upon which the one used by Jokinen is based. Briefly, air flow was sampled into the ionization region via a 1.9 cm ID stainless steel sampling tube. Inside the ionization region, a flow of air is introduced which surrounds the stainless steel sampling tube. This flow of air, termed the sheath flow, had been filtered to remove any SO_2 and "spiked" with a small amount (~10^{11} molecule cm^{-3}) of HNO_3. Upon entering the ionization region, the outer coaxial layer of sheath air was ionized by passing it over a 0.635 cm wide piece of ^{241}Am foil mounted on a 3.8 cm ID stainless steel tube concentric with the 1.9 cm tube. The ^{241}Am alpha source (~5 MeV) was positioned so as to minimize ionization of the sample flow, and ensure that the initial ionization remain confined to the outer sheath flow region. As the sheath flow passes over the ^{241}Am source, the added HNO_3 is ionized in a multi-step process to form $NO_3^- \cdot (HNO_3)_n$ reagent ions (n=0,1,2). The $NO_3^- \cdot HNO_3$ ions are used as the primary reagent ion instead of NO_3^- or $NO_3^- \cdot (HNO_3)_2$ because the sampled air can have a sufficient concentration of HNO_3 to convert NO_3^- formed in the ion source into $NO_3^- \cdot HNO_3$ (Tanner et al., 1997). Exiting the ion source region the $NO_3^- \cdot (HNO_3)_n$ ions, but not the gas in which they were formed, are directed by means of electrostatic lenses (V=-135V) through the intermediate, un-ionized, annular layer of sheath gas into the central sample flow. Once in the sampled air flow, the $NO_3^- \cdot (HNO_3)_n$ reagent ions react with more acidic species, such as H_2SO_4, to produce product ions:

$$H_2SO_4 + NO_3^- \rightarrow HSO_4^- + HNO_3 \qquad\qquad\qquad (R1)$$

Alternatively, the NO_3^- ions can cluster with certain other species. The clustering reaction is particularly sensitive for highly oxidized compounds containing –OOH and -OH groups capable of forming hydrogen bonds with the nitrate ion (Rissanen et al., 2014; Hyttinen et al., 2015). For clarity, only the core ion species are shown in the above equation. At the end of the ion

reaction region the reagent and product ions are directed towards the vacuum system entrance by means of electrostatic fields (V=-123V).

H2SO4 is detected via its product ions, HSO4- (97 Th) and (HNO3)HSO4- (160 Th). It is the sum of these two peaks that is used in concentration calculations. Zero measurements were performed using a denuder and were less than 10^5 molecule cm^{-3}. The APi was tuned to minimize declustering of ions as they are directed to Tof region with pressures of 2.8 mbar and 0.04 mbar for SSQ 1 and 2 respectively. The ToF ran at an extraction frequency of 17 Hz.

2.2 OH Mode

The technique used here for the measurement of OH has been previously described (Eisele and Tanner, 1991; Eisele and Tanner, 1993; Tanner et al., 1997, Mauldin et al., 1998, Berresheim et al., 2000). Briefly, as the sample air flow is drawn in through the 1.9 cm inlet, a small amount (~3 x 10^{13} molecule cm^{-3}) of SO_2 is added to the flow through a pair of 0.023 cm ID transversely opposed injectors (Injector Pair #2) located near the front opening. The OH is then converted into H_2SO_4 via the reaction sequence:
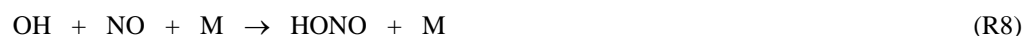
$$OH \; + \; SO_2 \; + \; M \; \rightarrow \; HSO_3 \; + \; M \qquad\qquad (R2)$$

$$HSO_3 \; + \; O_2 \; \rightarrow \; SO_3 \; + \; HO_2 \qquad\qquad (R3)$$

$$SO_3 \; + \; 2H_2O \; + \; M \; \rightarrow \; H_2SO_4 \; + \; H_2O \; + \; M \qquad\qquad (R4)$$

Previous quadrupole CIMS measurements of OH have incorporated the use of isotopically labeled $^{34}SO_2$ to allow the simultaneous measurement of naturally occurring H_2SO_4 as well as OH. Here, due to cost, unlabeled SO_2 was used as the reagent. The shortcoming of the use of the unlabeled SO_2 is the inability to measure ambient H_2SO_4 simultaneously while in the OH measurement mode. However, ambient H_2SO_4 concentrations are separately determined while in the NO_3^- mode. To prevent cycling of HO_2 and RO_2 back into OH, propane (an OH scavenger) is also added at much higher concentrations on a continuous basis through a second pair of injectors (Injector Pair #3) located ~5 cm downstream from the SO_2 injection. This propane removes any OH which has been cycled back from HO_2 and RO_2 via reactions with NO or O_3 after the ambient OH initially present has been converted into H_2SO_4. As in previous measurements (Eisele et al., 1991; Sjostedt et al., 2007) a small amount of HNO3 (~1x1012 molecule cm-3) was also added through the rear injectors to improve nitrate cluster distribution stability which directly affects instrument calibration. Once formed, the H_2SO_4 is detected via its product ion at masses 97 and 160 Th. To account for other non-OH oxidation processes that can also lead to H_2SO_4 formation from SO_2, a second measurement is made where ~1x10^{16} molecule cm^{-3} of propane is added together with the SO_2 through injector pair #2. This concentration is sufficient to scavenge >98% of the OH present via reaction with propane instead of SO_2. Hence, the concentration of OH is attributed to the difference between the total SO_2 oxidant signal (that with only SO_2 added through injector pair #2) and the non-OH SO_2 oxidant signal (with both propane and SO_2 added through injector pair #2). The source of the non-OH SO_2 oxidant signal has been found to follow the same characteristics as stabilized Criegee intermediates resulting from the ozonolysis of biogenic alkenes (Mauldin et al., 2012). Thus, this signal can be used to give an estimate of Criegee radical concentrations. However, contributions from other non-OH, non-Criegee species cannot be ruled out.

4

2.3 HO₂+RO₂ Mode

The measurement of HO_2+RO_2 incorporates the same technique as described by Cantrell et al., (2003) and Mauldin et al., (2004). Briefly, the technique involves the chemical conversion of peroxy radicals to H_2SO_4. As sampled air was drawn through the 1.9 cm ID inlet, a mixture of NO and SO_2 was added to the flow via a pair of injectors (Injector Pair #1).

5 Conversion of HO_2+RO_2 to H_2SO_4 then takes place via the following reaction sequence:

$$RO_2 + NO \rightarrow RO + NO_2 \tag{R5}$$

$$RO_2 + NO \rightarrow RONO_2 \tag{R5a}$$

$$RO + O_2 \rightarrow R'CHO + HO_2 \tag{R6}$$

$$HO_2 + NO \rightarrow OH + NO_2 \tag{R7}$$

10 $$OH + SO_2 + M \rightarrow HOSO_2 + M \tag{R2}$$

$$HOSO_2 + O_2 \rightarrow HO_2 + SO_3 \tag{R3}$$

$$SO_3 + 2H_2O \rightarrow H_2SO_4 + H_2O \tag{R4}$$

$$OH + NO + M \rightarrow HONO + M \tag{R8}$$

It is quite likely that some of the RO radicals produced in reaction R5 do not produce HO_2 from their reaction with O_2, but

15 do decompose to form measurable radicals (Cantrell et al., 2003). These radicals are rapidly transformed back to corresponding RO_2 radicals and thus may contribute doubly to the measured $[HO_2+RO_2]$. This increase however, is not expected to be particularly significant, as it is largely cancelled by reactions forming organo-nitrates through reaction 5a. This formation of organo-nitrates is especially important for the larger RO_2 radicals produced from terpene oxidation (Jokinen et al., 2014).

20 The above reaction sequence represents a chain reaction producing H_2SO_4, with OH reacting with either SO_2 in reaction R(2) to propagate the chain, or with NO in reaction R(8) which terminates the chain. The yield of H_2SO_4 per HO_2 is determined by the reaction time and the $[SO_2]/[NO]$ ratio (Cantrell et al., 2003). Larger $[SO_2]/[NO]$ ratios leads to a larger gain or increase in the concentration of H_2SO_4 per HO_2. In the current study the $[SO_2]/[NO]$ ratio was adjusted such that the gain of the system was ~1, i.e., each HO_2 produced, on average, one H_2SO_4 molecule. In the present study the SO_2 and NO

25 concentrations were ~300 ppbv and 50 ppbv, respectively. At still higher concentrations of NO (>1000 ppmv), the reaction of RO radicals via (2) is inhibited by the reaction:

$$RO + NO + M \rightarrow RONO + M \tag{R9}$$

This reaction has been exploited for purposes of measuring HO_2 only (not HO_2+RO_2) (Cantrell et al., 2003; Brune et al., 1995). In the current study, however, technical constraints prevented the use of such high concentrations of NO, limiting the

30 measurements to only HO_2+RO_2.

As in the case of the OH measurement, a second measurement is also performed to account for H_2SO_4 not produced from the conversion of HO_2. Here NO is added first (Injector Pair #1), and SO_2 is added 50 msec downstream of the NO addition (Injector Pair #2). NO is added in sufficient concentration such that 99% of the OH formed is converted to HONO before the

addition of the SO₂. To prevent any interference from NO in the OH or NO_3^- modes, the flow of the front pair of injectors (Injector Pair #1) is reversed to prevent any residual reagent gases from leaking into the sample flow.

2.4 Calibration

Two different methods are used to calibrate the system, both of which rely on water photolysis at 185 nm. In the field, calibration of the system is performed by producing a known amount of OH in front of the 1.9 cm sampling port (Tanner and Eisele, 1995; Tanner et al., 1997). This photolysis produces both OH and HO_2 via:

$$H_2O \; + \; h\nu \, (184.9 \, nm) \; \rightarrow \; OH \; + \; H \tag{R10}$$

$$H \; + \; O_2 \; + \; M \; \rightarrow \; HO_2 \; + \; M \tag{R11}$$

Light from a temperature controlled Hg lamp is reflected by two mirrors coated to selectively reflect the 184.9 nm emission line. The OH concentration produced by the calibration source is dependent upon the intensity (photo flux) at 184.9 nm, the [H_2O], the cross-section of H_2O at 184.9 nm, the yield of OH from H_2O photolysis, and the sample flow velocity. The flow velocity in the 10.1 cm duct was measured using a hotwire anemometer and the [H_2O] was measured by a hygrometer. A value of 7.2 x 10^{-20} cm^2 $molecule^{-1}$ was used for the absorption cross-section of H_2O at 184.9 nm (Cantrell et al., 1997), and the OH yield from the photolysis at 184.9 nm is ~100% (Baulch et al., 1982). Photon flux at 184.9 nm was mapped out using a vacuum UV diode mounted on an x/y movable drive. This diode was intercompared with a National Institute of Standards and Technology (NIST) standard diode before and after the study.

Calibration of the HO_2+RO_2 system was performed using the same system as for OH and H_2SO_4. Again, the amount of HO_2 produced is a function of the ambient H_2O, the Hg Pen Ray lamp flux at 184.9 nm, and the sample flow velocity. As both the OH and HO_2 are converted into H_2SO_4 via reactions (2-7), when in the HO2+RO2 mode, the resulting calibration coefficient is for the sum of OH and HO_2. If, therefore, the gain of the system is ~1, the calibration value should be approximately twice that for OH and H_2SO_4. Hence, this determination serves as both a calibration of the HO_2+RO_2 measurement as well as the gain of the system. The average calibration coefficient for HO_2+RO_2 obtained during the study was (5.63±0.67) x 10^9 molecule cm^{-3}, and the coefficient for OH and H_2SO_4 was (5.24±0.46) x 10^9 molecule cm^{-3}. These values indicate that the gain of the system was very close to one during study. It should be noted that these values are comparable to those previously obtained using a quadrupole system (Petäjä et al., 2009) indicating that the chemical conversion/ion reaction system was performing in a similar manner.

While not used in the field for this study, the OH and H_2SO_4 measurement can also be calibrated by a system that uses H_2O photolysis in presence of SO₂, to produce a known amount H_2SO_4 (Kürtén et al., 2012). In the past, this calibration system has produced similar values for the calibration coefficient (5-6) x 10^9 molecule cm^{-3} for a similar inlet configuration. Using this calibration coefficient, the calculated limit of detection for the OH measurement is ~2 x 10^5 molecule cm^{-3}, and ~2 x 10^6 molecule cm^{-3} for (HO_2+RO_2). The uncertainty in the current set of measurements is estimated at ± 40% for OH and

H_2SO_4. For $HO_2 + RO_2$ the uncertainty is somewhat larger, being $\pm 60\%$. The error value is 2σ and is calculated from a propagation of errors calculation which includes both the total systematic and random errors for a given measurement.

3 Results and Discussion

For the data presented here the instrument was run sequentially through the NO_3^- ion, OH, and HO_2+RO_2 modes. A sample trace of the measured H_2SO_4 concentration versus time for the three different measurement modes is shown in Figure 2. The data presented are un-averaged one second measurements, so that the response of the instrument to changes in modes can be clearly seen. At 13:08:30, the sequence begins with the instrument transitioning into the NO_3^- ion mode. As this transition simply involves switching a valve to draw ~100 sccm of flow from injector pair #1 and turning off the added reagent gases, it should be relatively fast. From the plot, it can be seen the H_2SO_4 concentration drops and stabilizes over the period of a 2-3 seconds to an average concentration of ~3.5 x 10^6 molecule cm^{-3}. The instrument remains in this mode for 240 sec. At ~13:12:30, the SO_2 and propane flows are then turned on and sent to injector pairs #2 and #3 respectively. This configuration is termed the OH "signal" mode, and the instrument remains in this mode for 30 sec. At this point propane is also added along with the SO_2 through injector pair #2 putting the instrument into the OH "background" mode. After 30 sec in this mode the instrument switches back to the OH "signal" mode. This switching between the OH "signal" and "background" modes continues for 240 sec allowing for four OH "signal" and "background" measurements to be obtained. Lines indicating the average H_2SO_4 concentration are also shown in the figure. The difference between the OH "signal" and "background" values is the concentration of H_2SO_4 attributed to production from OH. As can be seen from the figure, the SO_2 flow had not equilibrated for the first "signal" measurement and which is thus not used. From the data shown in Figure 3, the concentration of OH is ~3 x 10^6 molecule cm^{-3}. At this point propane is turned off, the NO flow turned on, the SO_2 flow adjusted, and valves switch such that NO and SO_2 are added through injector pair #1 putting the instrument into what is termed the HO_2+RO_2 "signal" mode. The instrument remains in this configuration for 30 sec at which point the SO_2 flow is switched so that it added through injector pair #2, putting the instrument into the HO_2+RO_2 "background" mode. After 30 sec in this mode the instrument switches back to the HO_2+RO_2 "signal" mode. This switching between the HO_2+RO_2 "signal" and "background" modes continues for 240 sec allowing for four HO_2+RO_2 "signal" and "background" measurements to be obtained. The difference between the HO_2+RO_2 "signal" and "background" values is the concentration of H_2SO_4 attribute to production from peroxy radicals. As can be seen from the figure, the SO_2 flow had not equilibrated for the first "signal" measurement and which is thus not used. From the data shown in Figure 3, the concentration of HO_2+RO_2 is (7-8) x 10^8 molecule cm^{-3}. At this point the measurement sequence is restarted by turning off all added reagents putting the instrument back into the NO_3^- ion mode. Using this measurement scheme, four 1 minute measurements of HO_2+RO_2, four 1 minute measurements of OH, and 240 sec of NO_3^- ion mode measurements are obtained every 12 minutes.

As stated above the combination of these techniques can yield additional information other than the measurement of the individual concentrations. Previous measurements of OH and HO_2+RO_2 employed the use of a quadrupole mass

spectrometer which requires measurements at specific masses (Hornbrook et al., 2011; Sjostedt et al., 2007; Mauldin et al., 2004; Cantrell et al., 1997; Eisele et al., 1991, 1993). The current HOxROx system uses HR-A detection which allows the entire mass spectrum to be recorded for each measurement. In addition to the measurement of H_2SO_4 during the NO_3^- mode, this feature has been used to measure numerous highly-oxidized multifunctional compounds (HOMs) (Ehn et al., 2014,

5   Rissanen et al. 2014, 2015, Jokinen et al 2014, Mentel et al 2015, Richters et al. 2016). The present use of the CI-APi-ToF during the OH or HO_2+RO_2 measurements allow one to see how these organic species behave when the sample flow is perturbed by the addition of SO_2 or NO.

Figure 3 show typical mass spectra obtained from the HOxROx instrument at the Hyytiälä research station. The major peaks have been labeled with their mass and the compounds they represent. The spectrum in Figure 3a was obtained while the

10   instrument was in the HO_2+RO_2 "signal" mode to better view the HSO_4^- (mass 97) and (H2SO¬4)NO_3^- (mass 160) product peaks. The high resolution of the CI-APi-ToF allows these product ions to be detected at their exact masses, 96.9601 amu and 159.9557 amu ensuring that they indeed were HSO_4^- and $(H_2SO_4)NO_3^-$ respectively. It can be seen that the reagent nitrate ion peaks; NO_3^-, $(HNO_3)NO_3^-$, and $(HNO_3)_2NO_3^-$, are the dominant peaks in the spectra. Even though the spectrum shown was obtained in the HO_2+RO_2 "signal" mode which produces the most product H2SO4, the reagent ion still

15   comprises ~97% of the total ion signal. The inset in the Figure illustrates the highly-oxidized products detected, with a few of the major identified product species labeled by their corresponding masses.

In Figure 3b a mass spectrum obtained while in the NO_3^- mode is presented. In this mode no reagents are added to the sample flow, which can be directly seen by the absence of the large product peaks at 97 and 160 Th. Also differences in the highly-oxidized product distribution at the higher masses are apparent and are illustrated in the inset of the Figure (i.e.,

20   compare the labelled peaks between the Figures a and b). Note especially the lower signal strengths of the masses 309 and 339 Th which have been previously identified as prominent organonitrates (Kulmala et al 2013). Both of these signals go up by addition of NO to the sample gas mixture, with a clear decrease in prominent radical signals (e.g., at 325 Th and 357 Th assumed to originate from MT ozonolysis, see Rissanen et al. 2015), indicating organonitrate formation through 5a and thus supporting the previous identification. Also the SO_2 addition is seen to modulate some of the HOM signals, but the reason

25   for this behavior is currently unclear. In Figure 4, a time series of H_2SO_4 together with other selected masses is shown. Larger values of H_2SO_4 are indicative of SO_2 addition from either the OH or HO_2+RO_2 measurement modes. From the plot it can be seen that the mass 309 is correlated and mass 340 is anti-correlated with the addition of SO_2 respectively. The mass 339 peak however shows a decrease with the initial addition of SO_2 (OH mode), but then returns close to its non- SO_2 value later in the measurement series during the HO_2+RO_2 mode where NO is also present. This modulation could be explained by

30   gas-phase organosulfur compound formation, potentially organoulfonates or organosulfates, but the mechanism behind this is presently unknown, as the organosulfur compounds are generally thought to originate from condensed phase reactions (Riva et al., 2016; Kramer et al., 2016).

In Figure 5 a time series of mass 325 along with the H_2SO_4 signal is shown. Mass 325 is mainly assumed to originate from a $C_{10}H_{15}O_8(NO_3^-)$ species - a nitrate cluster with a common organo-peroxy radical produced from the oxidation of

monoterpenes (e.g., α-pinene; Jokinen et al., 2014, Rissanen et al., 2015). These data are presented as one minute averages and include measurements from all three modes. It should be noted that the one minute averaging combines the OH and HO_2+RO_2 "signal" and "background" measurements such that they cannot be distinguished. By following the H_2SO_4 signal, however, it is possible to see when SO_2 is being added or not, with the lowest values corresponding to the NO3- ion mode

5   where no reagents are added. From the plot it is evident that both species are indeed modulated and anti-correlate with each other. The modulation arises from the instrument changing its mode of operation (NO_3^-, OH, or HO_2+RO_2). The anti-correlation indicates the conversion of RO_2 into H_2SO_4 during the HO_2+RO_2 portion of the measurement. By adding NO to the inlet the intermediate RO_2 radicals observed in the spectra should convert to corresponding alkoxy (RO) radicals and organic nitrates ($RONO_2$; reactions 5 and 5a, respectively), with the smallest radicals giving RO and the branching steadily

10   shifting in favor of nitrates as the molecular size increases. For the current ambient data set, the addition of NO lead to significant decreases in the RO_2's detected, but did not remove them quantitatively (Figure 5). One possible reason for this behavior could be that the NO addition is actually helping certain autoxidation pathways to proceed by creating alkoxy intermediates which promptly isomerize and thus advance the oxidation sequence (Kürtén et al. 2015, Mentel et al. 2015), and result in isomeric peroxy radical products detected at the same masses in the spectra.

15   The combination of quantifying the amount of direct (=OH) and indirect (=HO_2+RO_2) oxidants together with their specific low-volatile reaction products can be highly useful for gaining insight into atmospheric oxidation pathways, especially relating to SOA formation. The simultaneous quantification of the variation in the main day-time oxidizer, the OH radical, with the variation in the formation rate of highly-oxidized molecules will inform about the oxidation pathways, but also it can improve our knowledge on the limitations of this processes, e.g., is the HOM formation oxidant and/or VOC limited in

20   the environment under considerations by observing the correlation of these concentrations. While data in Figures 4 and 5 show clear correlations in the changes of the oxidized organics with the addition of reagent gasses, detailed analysis of the spectra to determine the correlations and mechanisms for the formation of these species is beyond the scope of this paper which mainly aims at providing a description of the advantage of using this novel combination of methods. These data are presented to demonstrate the potential extension that the combination of modes has to shed light on the chemical

25   mechanisms for the formation of these highly oxidized organic species. In particular, the combination of the addition of NO in the HO_2+RO_2 mode with information from the NO3- ion mode could elucidate formation pathways for HOM (and subsequently ELVOC) species proposed as crucial precursors to SOA formation. These compounds have been previously shown to form through sequential RO2 isomerization + oxygen addition reactions leading to end products with multiple carbonyl, hydroperoxy and peroxyacid functionalities (Crounse et al., 2013; Rissanen et al., 2014; Mentel et al., 2015). Some

30   of the peroxy intermediates are directly detected by clustering with NO3- ions (e.g., Mentel et al., 2015 and Richters, et al. 2016) and thus they should also be susceptible to manipulation with the addition of gas-phase reagents. These types of analysis together with further laboratory investigations are ongoing and will be presented in future publications.

4 Conclusions

A new HO_xRO_x instrument has been constructed which combines the previously used chemical conversion techniques for the detection of OH, and HO_2+RO_2 together with NO_3^- ion chemical ionization and High Resolution-Time of Flight mass detection. The instrument has the ability to switch between modes which measure OH and HO_2+RO_2 where chemical reagents are added to the sample flow, and a NO_3^- ion mode where no reagents are added to the flow. All three modes utilize CI-APi-ToF mass detection, which, unlike previous measurements of OH or HO_2+RO_2, allows the entire mass spectrum to be recorded with each measurement. To the authors knowledge this is the first use of a CI-APi-ToF for OH or HO_2+RO_2. Calibration coefficient values were comparable to those obtained using a quadrupole system. Similar calibration factors were measured for OH and HO_2+RO_2, which shows that the HO_2+RO_2 measurement was operated with a gain of one (i.e. one H_2SO_4 produce for each HO_2 or RO_2 reacted). Thus, by switching modes, an entire suite of oxidation products (H_2SO_4 and HOMs) can be measured along with the concentrations of OH and HO_2+RO_2 with one instrument. While the use of one instrument to obtain these individual measurements is of practical value, it is the combination of this information that extends the value beyond that of the measurements themselves. The manipulation of the inlet chemistry via the addition of gas-phase reagent species can perturb oxidation processes allowing additional information to be gained on chemical pathways and mechanisms.

5 References

Baulch, D.L., Cox, R.A., Crutzen, P.J., Hampson Jr., R.F., Kerr, J.A., Troe, J., Watson, R.T., Evaluated kinetic and photochemical data for atmospheric chemistry supplement/CODATA task group of chemical kinetics, J. Phys. Chem. Ref. Data, 11, 377, 1982.

Berresheim H., Elste T., Plass-Dülmer C., Eisele F.L., Tanner D.J., Chemical ionization mass spectrometer for long-term measurements of atmospheric OH and H_2SO_4, Int. J. Mass Spectrom., 202, 91–109, 2000.

Brune, W. H., Stevens, P. S., Mather, J. H., Measuring OH and HO_2 in the troposphere by laser-induced fluorescence at low pressure, J. Atmos. Sci., 52, 3328-3336, 1995.

Cantrell, C.A., Tyndall, G., Zimmer, A., Absorption cross-section for water vapor from 183 to 193 nm, J. Geophys. Res., 24, 2195-2198, 1997.

Cantrell, C. A., Edwards, G. D., Stephens, S., Mauldin, L., Kosciuch, E., Zondlo, M., Eisele, F., Peroxy radical observations using chemical ionization mass spectrometry during TOPSE, J. Geophys. Res., 108, 8371, 2003.

Crounse, J.D., Nielsen, L.B., Jogensen, S., Kjaergaard, H.G., P.O. Wennberg, Autoxidation of Organic Compounds in the Atmosphere, J. Phys. Chem.Lett., 4, 3513-3520, 2013.

Edwards G.D., Cantrell, C.A., Stephens, S., Hill, B., Goyea, O., Shetter, R.E., Mauldin, R.L., Kosciuch, E., Tanner, D.J., Eisele, F.L., Chemical ionization mass spectrometer instrument for the measurement of tropospheric HO2 and RO2, Anal. Chem., 75, 5317-5327, 2003.

Ehn, M., et al., Mass spectrum of ELVOCs produce by a-pinene ozonolysis, Nature, 506, 476-479, doi:10.1038/nature 13032, 2014.

Eisele, F.L., and Tanner, D.J., Ion-assisted tropospheric OH measurements, J. Geophys. Res., 96, 9295-9308, 1991.

Eisele, F.L., and Tanner, D.J., Measurement of the gas phase concentration of H_2SO_4 and methane sulfonic acid and estimates of H_2SO_4 production and loss in the atmosphere, J. Geophys. Res., 98, 9001-9010, 1993.

Heard, D. E., and Pilling, M. J. Measurement of OH and HO_2 in the troposphere, Chem. Rev., 103, 5163-5198, 2003.

Hornbrook, R.S., Crawford, J.H., Edwards, G.D., Goyea, O., Mauldin, R.L., Olson, J.S., Cantrell, C.A., Measurements of tropospheric HO2 and RO2 by oxygen dilution modulation and chemical ionization mass spectrometry, Atm. Meas. Tech., 4, 735-756, 2011.

Hyttinen, N., Kupianen-Maatta, O., Rissanen, M.P., Muuronen, M., Ehn, M., Kurten, T., Modeling the Charging of Highly Oxidized Cyclohexene Ozonolysis products Using Nitrate Based Chemical Ionization, J. Phys. Chem. A, 119, 6339-6345, 2015.

Jokinen, T., Sipilä, M., Junninen, H., Ehn, M., Lönn, G., Hakala, J., Petäjä, T., Mauldin III, R.L., Kulmala, M., Worsnop, D.R., Atmospheric sulphuric acid and neutral cluster measurements using CI-APi-TOF. Atmos. Chem. Phys. 12: 4117–4125, 2012.

Jokinen, T., Sipilä, M., Richters, S., Kerminen, V.-M., Paasonen, P., Stratmann, F., Worsnop, D., Kulmala, M., Ehn, M., Herrmann, H., Berndt, T., Rapid Autoxidation Forms Highly Oxidized RO_2 Radicals in the Atmosphere. Angew. Chem. Int. Ed., 53: 14596–14600. doi: 10.1002/anie.201408566, 2014.

Kramer, A.J., Rattanavaraha, W., Zhang, Z.F., Gold, A., Surratt, J.D., Lin, Y.H., Assessing the oxidative potential of isoprene-derived epoxides and secondary organic aerosol, Atm. Environ., 130, 211-218, 10.1016/j.atmosenv.2015.10.018, 2016.

Kürtén, T., Rissanen, M. P., Mackeprang, K., Thornton, J. A., Hyttinen, N., Jørgensen, S., Ehn, M., and Kjaergaard, H. G., A Computational Study of Hydrogen Shifts and Ring-Opening Mechanisms in α-pinene Ozonolysis Products, J. Phys. Chem. A, 119 doi: 10.1021/acs.jpca.5b08948, 2015.

Kürtén A., Rondo L., Ehrhart S. & Curtius J., Calibration of a chemical ionization mass spectrometer for the measurement of gaseous sulfuric acid. J. Phys. Chem. A, 116, 6375–6386, 2012.

Mauldin, R.L. III, Tanner, D.J., Frost, G.J., Chen, G., Prevot, A.S.H., Davis, D.D., Eisele, F.L., OH measurements during ACE-1: observations and model comparisons, J. Geophys. Res., 103, 16713-16729, 1998.

Mauldin, R.L., Kosciuch, E., Henry, B., Eisele, F.L., Shetter, R., Lefer, B., Chen, G., Davis, D., Huey, G., Tanner, D., Measurements of OH, HO_2+RO_2, H_2SO_4, and MSA at the South Pole during ISCAT 2000, Atmos. Environ., 38 (32), 5423-5437, 2004.

Mauldin, R. L. III, Berndt, T., Sipilä, M., Paasonen, P., Petäjä, T., Kim, S., Kurtén, T., Stratmann, F., Kerminen, V.-M., Kulmala, M., A new atmospherically relevant oxidant of sulphur dioxide, Nature, 488, 193–196, 2012.

Mentel, T. F., Kleist, E., Andres, S., Dal Maso, M., Hohaus, T., Kiendler-Scharr, A., Rudich, Y., Springer, M., Tillmann, R., Uerlings, R., Wahner, A., Wildt, J., Secondary aerosol formation from stress-induced biogenic emissions and possible climate feedbacks, Atm. Chem. Phys., 13, 8755-8770, DOI: 10.5194/acp- 13-8755-2013, 2013.

Petäjä, T., Mauldin, R.L., Kosciuch, E., McGrath, J., Nieminen, T., Paasonen, P., Boy, M., Adamov, A., Kotiaho, T., Kulmala, M., Sulfuric acid and OH concentrations in a boreal forest site. Atmospheric Chemistry and Physics, 9, 7435-7448, DOI: 10.5194/acp-9-7435-2009, 2009.

Richters, S., Herrmann, H., Berndt, T., Highly Oxidized RO2 Radicals and Consecutive Products from the Ozonolysis of Three Sesquiterpenes, Environ. Sci. Tech., 50, 2354-2362, 10.1021/acs.est.5b05321, 2016.

Rissanen, M.P., Kurten, T., Sipilä, M., Thronton, J.A., Kangasluoma, K., Sarnela, N., Junninen, H., Jorgensen, S., Schallhart, S., Kajos, M.K., Taipale, R., Springer M., Mentel, T.F., Ruuskanen, T., Petäjä, T., Worsnop, D.R., Kjaergaard, H.G., Ehn, M., The Formation of Highly Oxidized Multifunctional Products in the Ozonolysis of Cyclohexene, Am. Chem. Soc., 136, 15596-15606, 2014.

Rissanen, M. P., Kurtén, T., Sipilä, M., Thornton, J. A., Kausiala, O., Garmash, O., Kjaergaard, H. G., Petäjä, T., Worsnop, D. R., Ehn, M., and Kulmala, M., Effects of Chemical Complexity on the Autoxidation Mechanisms of Endocyclic Alkene Ozonolysis Products: From Methylcyclohexenes toward Understanding α-Pinene, J. Phys. Chem. A, 119, 4633–4650, 2015.

Riva, M., Budisulistiorini, S.H., Zhang, Z.F., Gold, A., Surratt, J.D., Chemical characterization of secondary organic aerosol constituents from isoprene ozonolysis in the presence of acidic aerosol, Atm. Environ., 130, 5-13, 10.1016/j.atmosenv.2015.06.027, 2016.

Sjostedt, S. J., Huey, L. G., Tanner, D. J., Peischl, J., Chen, G., Dibb, J. E., Lefer, B., Hutterli, M. A., Beyersdorf, A. J., Blake, N. J., Blake, D. R., Sueper, D., Ryerson, T., Burkhart, J., Stohl, A., Observations of hydroxyl and the sum of peroxy radicals at Summit, Greenland during summer 2003, Atmos. Environ., 41, 5122–5137, doi:10.1016/j.atmosenv.2006.06.065, 2007.

Tanner, D.J., and Eisele, F.L., Present OH measurement limits and associated uncertainties, J. Geophys. Res., 100, 2883-2892, 1995.

Tanner, D.J., Jefferson, A., Eisele, F.L., Selected ion chemical ionization mass spectrometric measurement of OH, J. Geophys. Res., 102, 6415-6425, 1997.
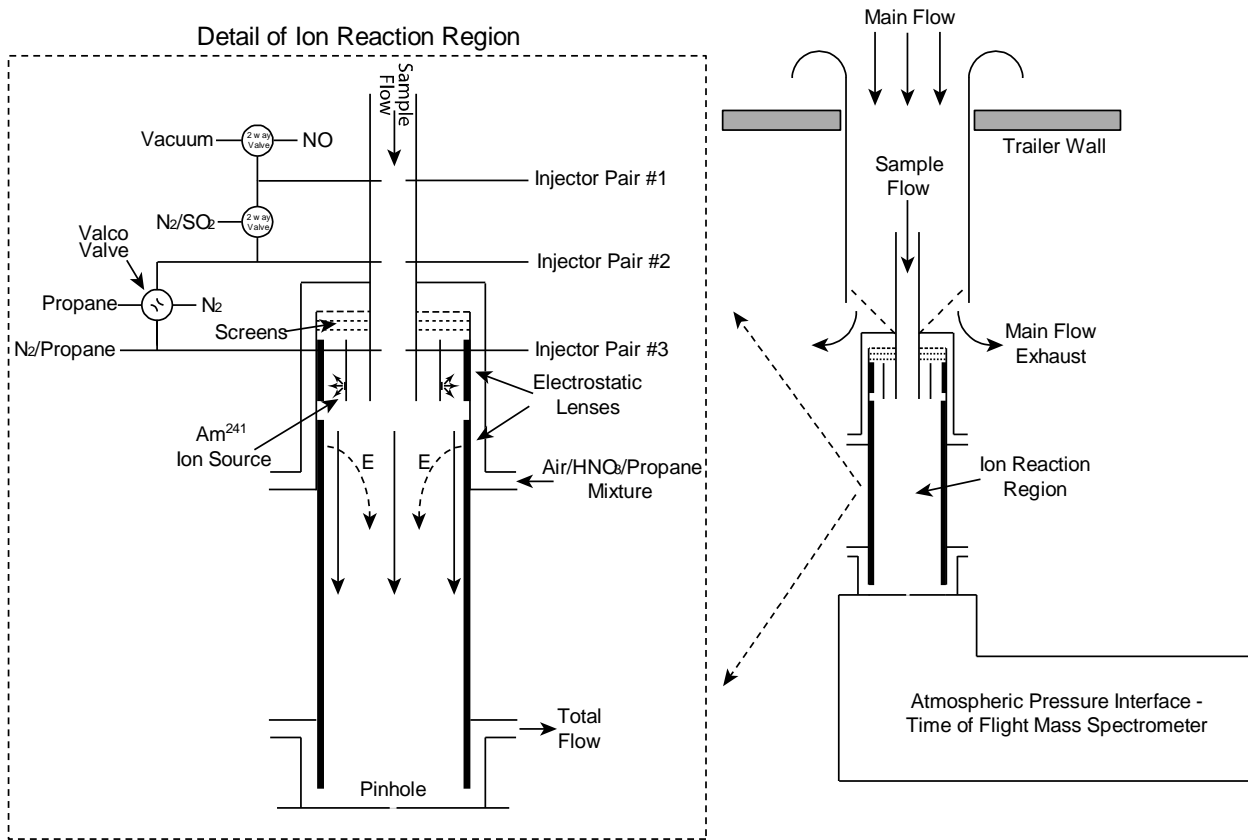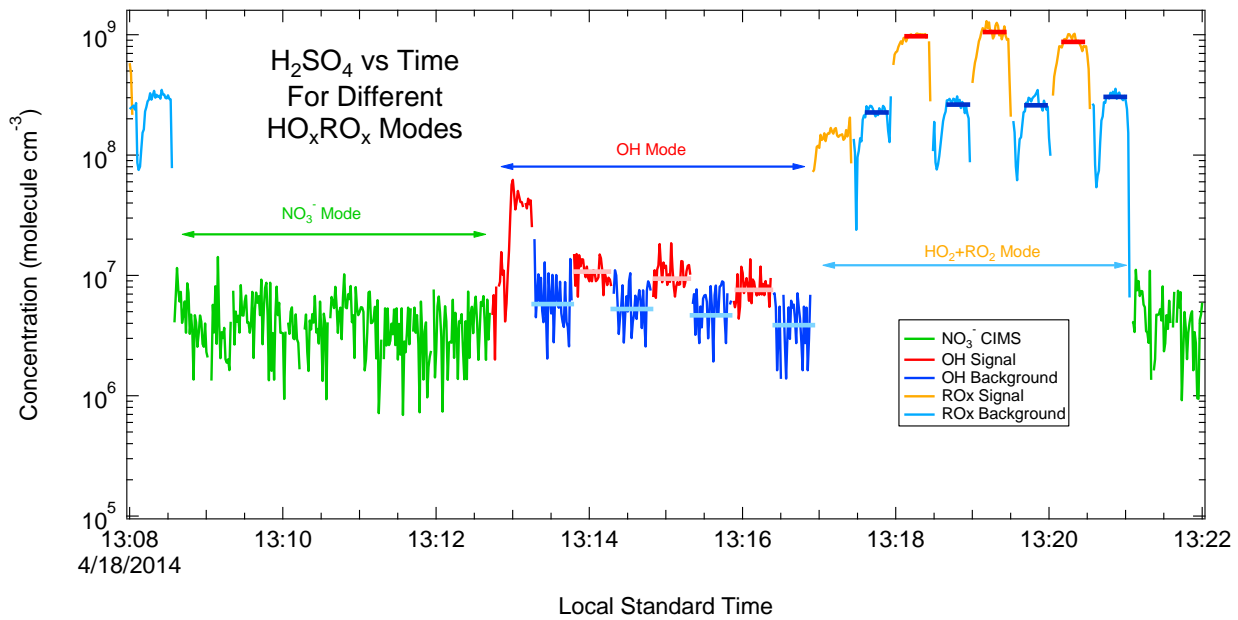
Figure 1 – Schematic of HOxROx Instrument

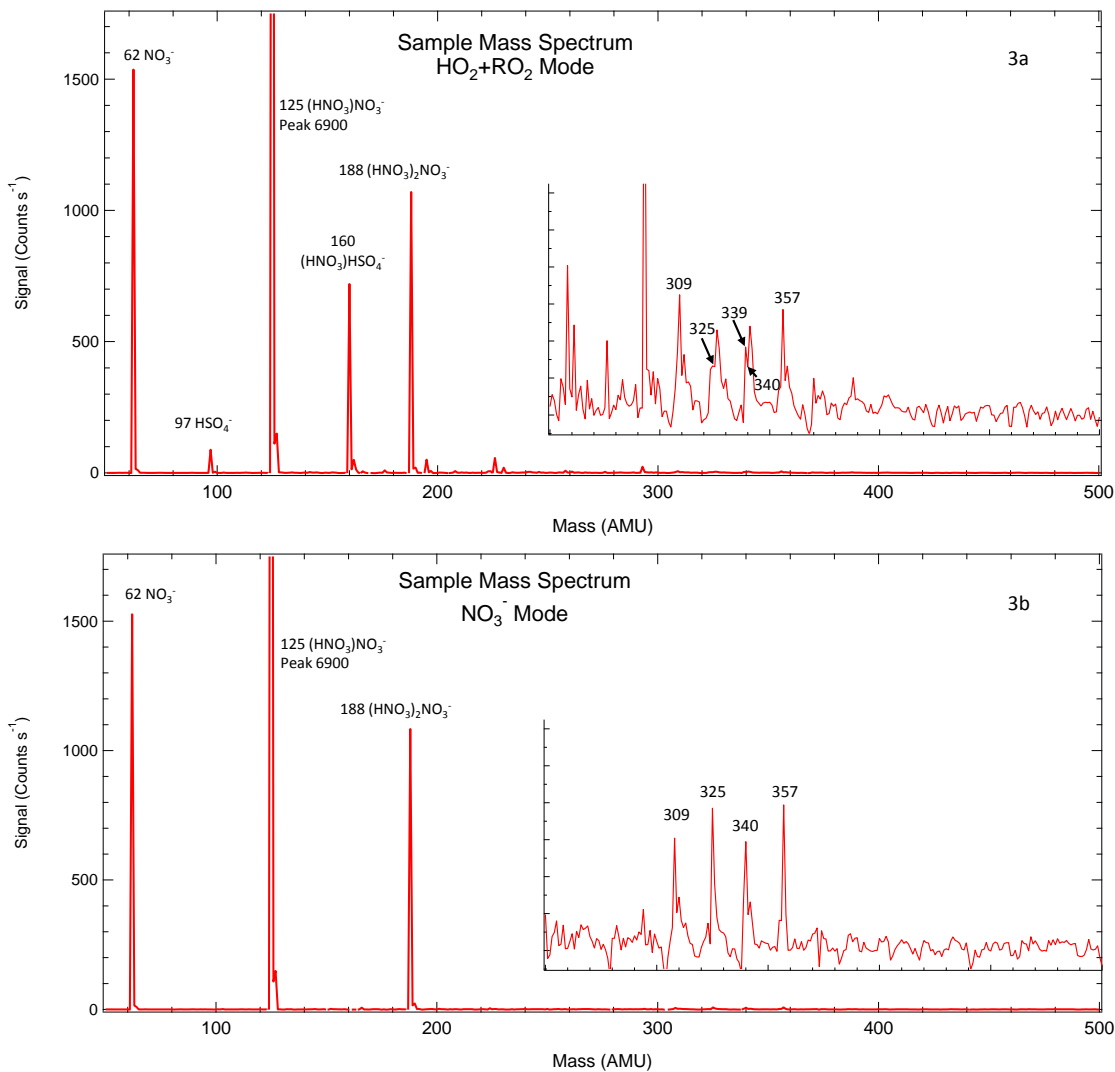Figure 2 – Time series of H₂SO₄ concentrations from different HOxROx modes.

5

Figure 3 – Sample ambient mass spectrum obtained at the Hyytiälä research station together with peak assignments. In 3a, the instrument is in the HO2+RO2 mode, while in 3b it is in NO3- mode. The insets are expanded views of the portion

5   below. Note the changes between modes in the peaks at 325 Th and 357 Th, radical signals assumed to originate from MT ozonolysis (see text).
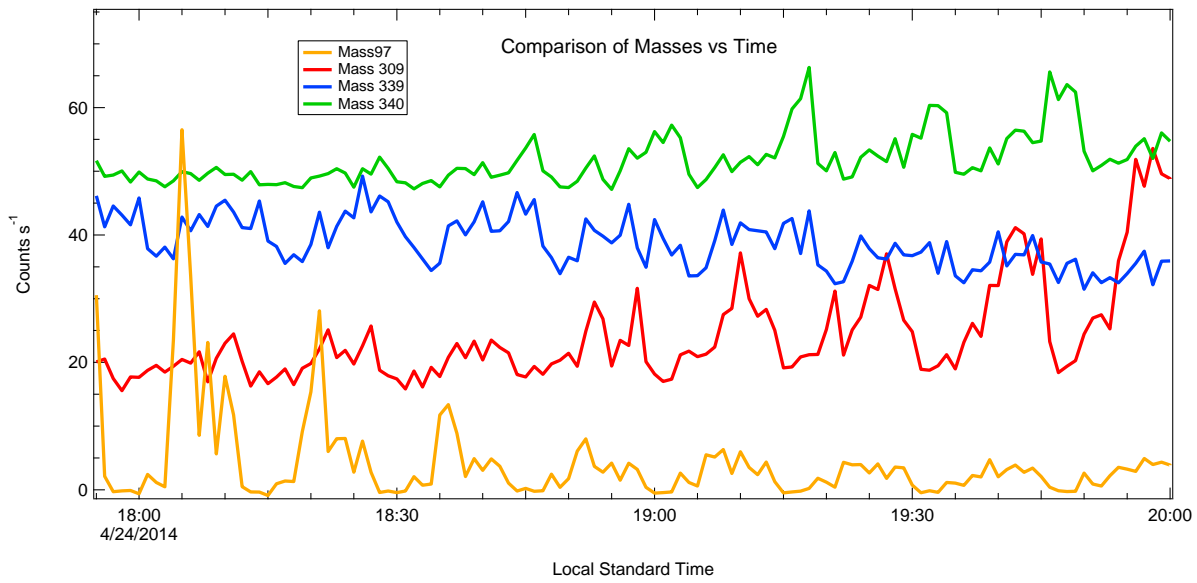
Figure 4 – Time series of H_2SO_4 and other selected masses obtained with the HO_xRO_x instrument. Traces have been offset for clarity.
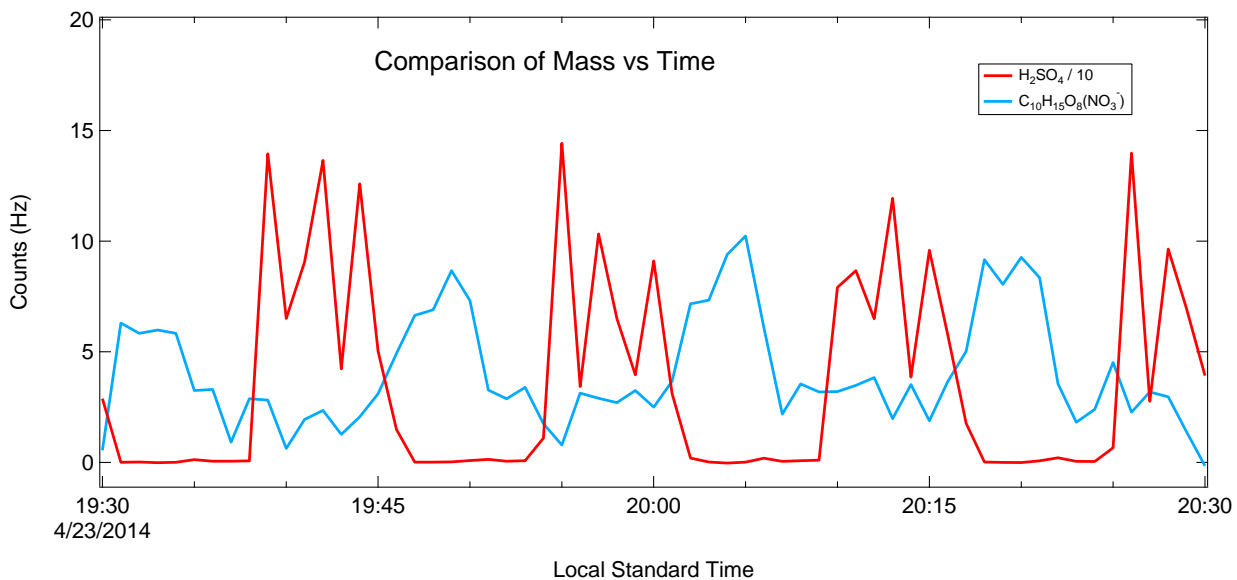
5

Figure 5 – Time series of H_2SO_4 and $C_{10}H_{15}O_8(NO_3^-)$ (mass 325). $C_{10}H_{15}O_8(NO_3^-)$ is a common organo-peroxy radical resulting from $\square$-pinene oxidation. As can be seen, both traces are modulated and anti-correlated. The modulation arises from changes in the mode of operation of the instrument (NO_3^-, OH, or HO_2+RO_2). The anti-correlation indicates the conversion of RO_2 into H_2SO_4 during the HO_2+RO_2 portion of the measurement.